Rumination on Design and Build of an ASTM D-5470 Thermal Interface Test Instrument

C. T. MURRAY, P. KENDALL, A. LARSON, C. HARVEY
and G. STAUS

ABSTRACT

In this paper we will present work-to-date on an ASTM D-5470 standard apparatus where we have tried to incorporate improvements implemented or suggested by other authors [1,2,3,4]. These improvements, in the past, have included increasing the heat flux capability of the device, improving the temperature measurement and thermocouple hole location accuracy, improvement of the parallelism, and improvement in measurement of the thickness of the interface material. Our main focus with this design has been on increasing the heat flux of the apparatus and implementing an optical system for gap measurement and parallelism adjustment.

INTRODUCTION

Thermal interface materials (TIMs) are thermally conductive solids and liquids used to thermally connect a hot object with a cooling source. Microprocessor applications involving the coupling of the Central Processing Unit (CPU) or other integrated circuits with a heat sink are increasing in heat flux and require lower impedance TIMs.

The ASTM D-5470 test method is a standard method to measure thermal impedance for TIMs such as elastomers, tapes, greases and phase change materials. As the TIM impedance drops with new materials there is a need for the ASTM tester to become more sensitive. The new version of the test making its way through ASTM will correct some of the historical legacies such as the high pressure requirement. The ASTM test defines thermal impedance, θ, to include the thermal

Cameron T. Murray, 3M EMMD, 251-2A-08, St. Paul MN 55144

resistance of the material ($\theta_{material}$) plus the interfacial contact resistance of the TIM to the substrates ($\theta_{interface}$);

$$\theta_{total}\ (\text{K-cm}^2/\text{W}) = \theta_{material} + \theta_{interface} \quad (1)$$

The one dimensional heat flow Fourier's Law defines the thermal impedance of a material as:

$$\theta_{material} = \Delta T \bullet A / Q = t/k_{bulk} \quad (2)$$

Where ΔT is the temperature difference across the TIM under test from the hot meter bar to the cold meter bar, A is the area of the meter bars, t is the thickness of the sample, and k_{bulk} is the material bulk conductivity. Combining equations 1 and 2,

$$\theta_{total}\ (\text{K-cm}^2/\text{W}) = \theta_{interface} + t/k_{bulk} \quad (3)$$

The method for separating $\theta_{material}$ from $\theta_{interface}$ is to measure θ_{total} as a function of thickness [5]. This plot is linear and the slope of the line is proportional to $1/k_{bulk}$, and the intercept is a measure of $\theta_{interface}$.

The main improvement in the past for the ASTM D5470 test has been obtaining a more accurate measurement of the ΔT, either by temperature measurement improvements [3] or by increasing the heat flux [1,2], or both. Our approach has been to work on increasing the heat flux while using reasonably accurate temperature measurements. Rearranging equation 2 we want to measure the heat flux, Q, required for a fixed ΔT,

$$Q = \Delta T \bullet A/\theta_{material} \quad (4)$$

Figure I illustrates two heat flux vs. $\theta_{material}$ curves calculated from equation 4, arbitrarily assuming either 2 K or 5 K ΔT is desired for low error in the temperature measurement. The highest performing TIMs are some of the low melting indium based metal alloys with a reported resistance of 0.06 K-cm^2/W [1]. These TIMs would require a heat flux of 76 W/cm^2 (for a 5 K ΔT) or 30 W/cm^2 (for a 2 K ΔT). Previous work has calculated the percent error as a function of heat flux and also found significant reduction in error for low impedance TIMs with increasing heat flux [1]. We attempted to design a system capable of heat fluxes greater than 50 W/cm^2, which also happens to correspond to the heat fluxes of current production CPU's [6].

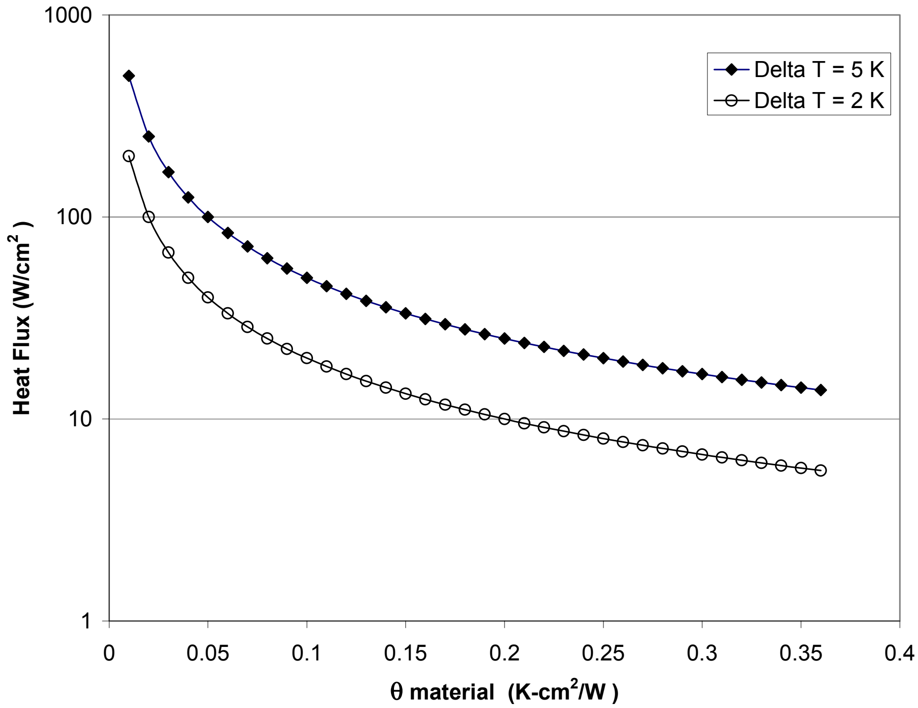

FIGURE I. HEAT FLUX REQUIREMENTS FOR FIXED ΔT

DESIGN CONSIDERATIONS

General Layout

All D-5470 devices, at their core, are two metal bars (meter bars) which are placed between a heater and colder source separated by the specimen to be tested. The test method permits latitude in the basic design while defining the smoothness of the meter bars in an attempt to minimize interfacial impedance between the meter and the specimen and to improve machine to machine agreement [5,7].

The overall dimension of this apparatus is 4 ft by 4 ft (1.2 m x 1.2 m) for the solid aluminum base. The y-plate is about 16 inches (40 cm) off the base. Two CAD views of this device are shown in Figures II and III. The two meter bars are in the center of a much larger support structure. This design implements a camera system to measure marks on the meter bars from three sides to obtain gap and parallelism information. To obtain accurate adjustment of bar parallelism the design uses the large Y shaped support plate which tilts the upper meter bar from three pivot points using turnbuckles. These turnbuckles give each support point the equivalent of greater than 200 thread-per-inch (80 thread-per-cm) adjustment screw.

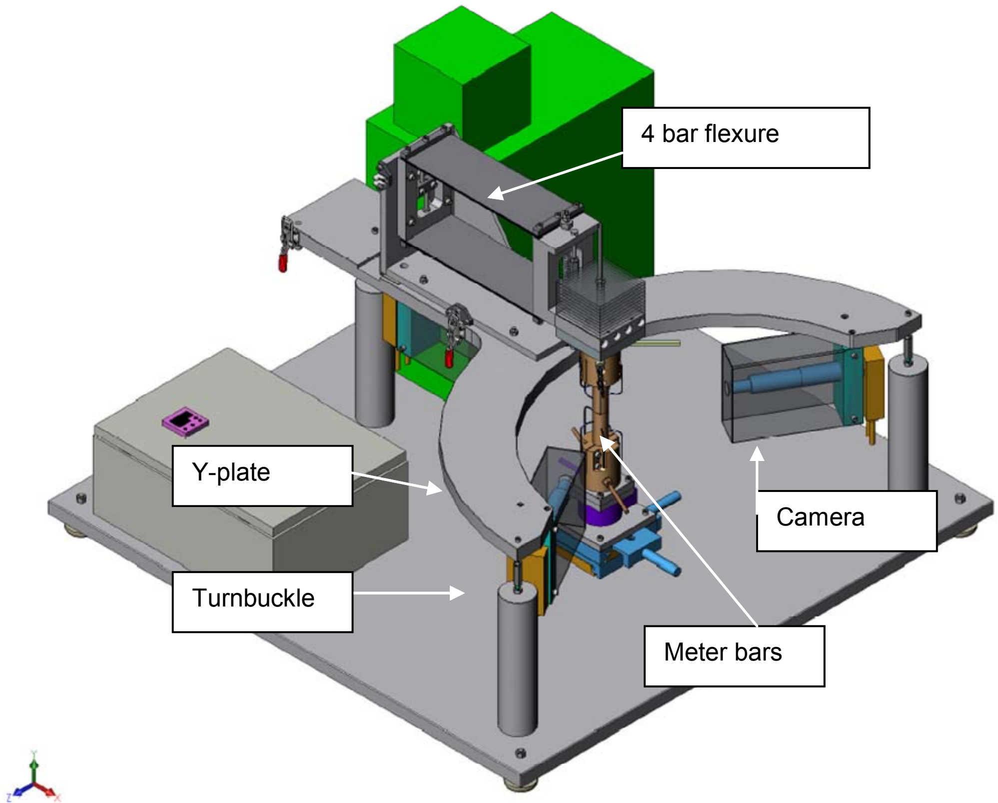

FIGURE II. SCHEMATIC OF ASTM D-5470 APPARATUS, WIDE VIEW.

The meter bars are connected to the heater cartridge and the cooling fluid via a copper block clamping fixture. The bottom meter bar (cold bar) has an x-y translation table and a load cell to measure the applied force which is applied using dead weights sitting on a small platform above the hot bar fixture. There is no guard heater in this design.

We can raise and lower the top meter bar about 1 inch without loss of top bar angle relative to the lower bar, through use of a four-bar flexure assembly. In addition the hot meter bar can be raised beyond 1 inch with a hinge at the rear of the four-bar flexure assembly.

Increased heat flux

Heat is supplied by the main cartridge heater which is mounted in the top of the hot side copper block clamping fixture. The hot block temperature is set with controllers and thermocouples separate from the resistance thermometer detection (RTD) measurement system. The heat flux is defined as the power per unit area. Since the area is proportional to the square of the diameter of the bar, reducing the meter bar diameter has a large effect upon the heat flux. In our design we selected a 25 mm diameter meter bar and a 300 W cartridge heater which would yield a theoretical 61 W/cm^2 assuming no heat losses and full power applied [8]. The cold bath also has to be selected to remove sufficient heat, and we chose a refrigerated/heating circulator capable of 350 W of cooling at 20 °C [9].

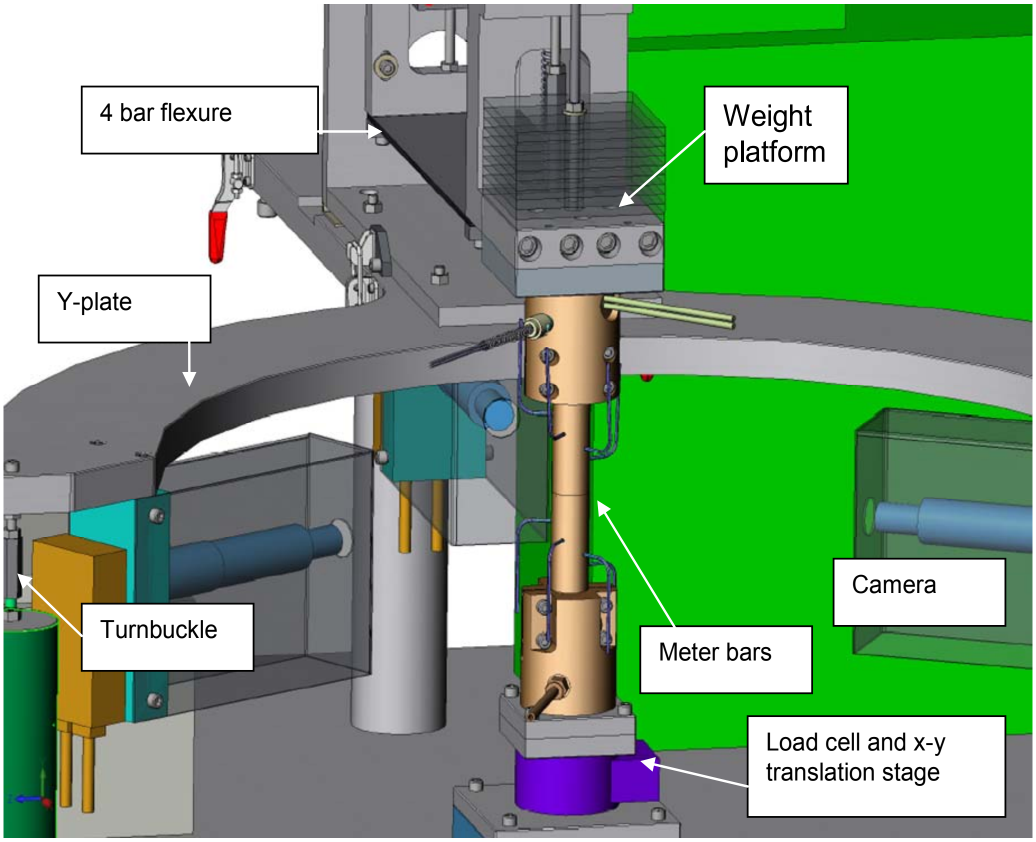

FIGURE III. SCHEMATIC OF THE ASTM D-5470 APPARATUS, CLOSE VIEW.

We selected Copper alloy 110 meter bars because of their high bulk conductivity [10]. The approximate value of k_{meter} for these bars is around 395 W/m-K, but one should use the values for the temperature of the meter bar during test. Maximizing the meter bar conductivity also maximizes the heat flux (see Equation 5).

Temperature measurement

Other papers have outlined several methods for measuring the temperatures as accurately as possible [1,2,3,4] including the use of Resistance Temperature Detectors (RTDs) instead of thermocouples. In addition the RTD holes locations need to be very accurately determined and normal to the meter bar. The fit between the RTD and hole should be tight, possibly with a thin layer of thermal grease to ensure good contact. Wrapping the RTD wires around the meter bar at the RTD elevation and insertion of the thermocouple deep the substrate to minimize heat loss out the lead wires has been demonstrated [3] so we adopted this design (Figure IV shows unwrapped RTDs to highlight the RTD hole locations).

In our instrument there are 5 RTDs uniformly spaced at 10 mm intervals in a spiral pattern in both the cold and hot meter bars, as shown in Figure IV. The closest RTDs are 8 mm from the test surface. The RTDs are 0.095 in diameter by 0.5 in long with 316 stainless steel sheaths [11]. The RTD sensors are centered across the diameter of the meter bar in their holes. The RTDs, closest to the heat/cold sources are located at least 14 mm from the clamping point which should be sufficient to ensure uniform heat flux.[1]. We used a 4 wire resistance measurement using a National Instruments NI-4351 High Precision DAQ interface (5½ digit analog input, 24 bit

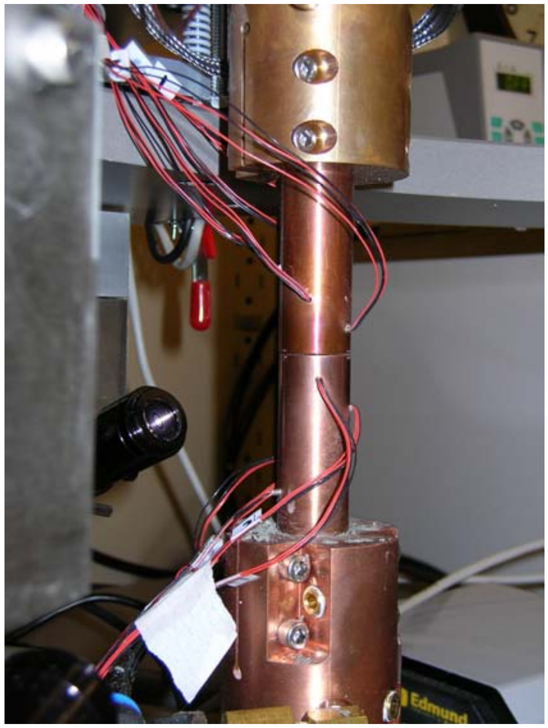

FIGURE IV. PHOTOGRAPH OF THE UNWRAPPED METER BARS

ADC). We purchased 100 ohm platinum film RTDs where each individual RTD resistance-temperature curve was measured [11]. Instead of using a custom calibration curve for each RTD we are using the NI-4351 DIN 43760 conversion table [12] for all RTDs. The error arising from this use of a standard curve is at most 0.15 °C at 100 °C [calculation provided by reference 11].

This design measures the temperatures in the meter bars to determine the heat flux, and to extrapolate the temperature to the surface of the meter bar in contact with the specimen. The heat flux in the experiment is determined from the slope of this temperature gradient dT/dx (K/m) and a known conductivity of the meter bar k_{meter} (W/m-K) material as;

$$Q = dT/dx \bullet k_{meter} \tag{5}$$

The surface temperature is obtained from the extrapolation of the plot of temperature vs. position to the zero position (or surface) of the meter bar. Using Excel and a Monte-Carlo simulation add-on we calculated the statistical error in calculation of the slope and surface intercept given the accuracy of the RTDs using a total error of ± 0.15 °C (current accuracy of DAQ system using common RTD calibration) The model calculation uses a copper meter bar with a 31 W/cm^2 heat flux. Ten thousand calculations are done randomly assigning a temperature (within the total error) to the RTDs. The calculation result is a maximum error of ± 0.14 °C in each meter bar surface temperature and a maximum error of ± 0.04 °C/mm in calculation of the slope (heat flux). A temperature slope error of 0.04 translates into 1.57 W/cm^2 heat flux error (using the 120 °C value of 393 W/m-K for k_{meter} from reference 10).

With the RTD holes we also have to consider the positional accuracy of our RTDs [4], and any influence the holes might have on the heat flow through the bar [3]. We believe the design elements of a spiral arrangement and a 10 mm height separation results in minimal heat flux distortions. Previous modeling shows that the heat flux returns to uniform about 1.5 diameters away from the hole with copper meter bars [3]. To minimize errors associated with hole position accuracy, the holes are measured each time we refinish the surface of the meter with a Nikon MM-40 measuring microscope. This measurement has deviation of ±0.002 mm in measured hole center location. The relatively large holes are easy to drill near their desired location and without drill wander [4,5].

Meter Bar Insulation

We currently run our ASTM tester without insulation on the meter bars. We need to keep open a line of site to the pins for the gap measurement and the meter bars are quite small in diameter so there is not much room for insulation. Calculations of the heat loss for these bars results in an estimated natural convective heat loss of less than 4.0 W [13]. The assumption is that since we measure the heat flux directly using the temperature gradient of the meter bars, we have minimized the effect of convective heat loss on the accuracy of the experiment. In many direct heat flux measurement ASTM designs the apparatus is set up without insulation, although several authors have stressed the importance of insulation [1,3]. Our future testing will evaluate the effect of insulation.

Gap Measurement and Parallelism

The meter bars have three 21 mil pins press fit into 20 mil holes, located 1 mm from the surface at three evenly spaced positions around the diameter. Hot bar and cold bar pins are in view in profile by each of the three DVT 510 M vision system cameras fitted with Infinity 4 mm field of view lenses [14]. The image has resolution of 480 x 640 pixels with 256 levels of grey. There are fiber optic lights illuminating the pins from the side and the cameras are viewing the reflection of the light off the pins, with a very dark background, resulting in good contrast. The relative separation of the pins is determined using image analysis firmware built into the camera with user input parameters.

Calibration of the camera system involves calibration the pixel measurement of the camera to an actual distance using an Edmund Industrial Optics “EO Magnifier Quality Resolution Chart”. The cameras always measure the separation between the two pins and since the pins are not at the surface, a “null” distance must be determined. The null distance of the pins and the “ideal” parallelism is established in an experiment where the upper meter bar is removed from its fixture and placed on the lower meter bar with the pins aligned. At this point the top and bottom smooth surfaces contact and by definition are parallel to each other. The separation of the pins at this point is measured and becomes the null position. The null value is subtracted from the total pin separation during a real experiment to determine the gap between the surfaces.

Parallelism is obtained by adjustment of the turnbuckles before the start of each TIM experiment. The turnbuckles are adjusted so that the gap reading for all the cameras measure within the desired maximum deviation from average. Typically we are able to adjust the top meter bar to be within ± 5 microns of parallel.

EXPERIENCES SO FAR

We are in the early stages of a shake down cruise with this device. In this paper we would like to share the positive aspects and challenges of this particular design.

Temperature Measurement and Control

We run this instrument in a fixed temperature mode using the heater cartridge with a proportional band control around a fixed set point temperature. The heat flux will depend upon the actual impedance of the sample under test. The lower the impedance to heat flow of the sample, the more power required from the heater to maintain its temperature (thus the higher the heat flux "driven" through the sample). This mode allows us to use the hot and cold set points to pick the average temperature of test. A disadvantage is that this test is not performed at a constant heat flux, for each thickness of gap there is a unique heat flux as the resistance decreases with gap.

It is believed that the ± 0.28 °C surface temperature (± 0.14 possible for each surface) was adequate for this higher heat flux design because we are expecting an increase in the ΔT. A low melting, indium based, metal alloy with a 0.06 °C-cm^2/W resistance TIM in our 61 W/cm^2 heat flux should result in a ΔT of 3.94 °C.

Limited Force Capability

The force on a sample is provided by dead weights sitting on the platform. This design limits us to approximately 40 lbs of force (177 N). The next revision of ASTM D-5470 will permit low pressure measurement for samples, to better reflect the reality of applications [7]. Grease measurements on our tester occur with a force which is effectively zero for most gap settings. The grease squeezes out of the gap effectively relieving the force as seen by Solbrekken, et. al. [2]. Eventually the gap gets small enough (approximately 25 to 50 microns) that force builds up. Adding as much force as possible we continue to take measurements, but the greases show little decrease in thickness nor much reduction in impedance. The literature suggests that thermal greases do not perform linearly with gap as predicted by equation 3 [1,15]. If our instrument had higher pressure capability we might observe this effect, although these pressures are outside the desired force in standard applications.

Camera Imaging of the Gap

Overall this camera imaging has been a success; the cameras are capable of meeting our design goal. In one experiment we measured 111 data points taken over a 15 minute span for a sample with an average gap of 2141 (which is close to the full scale of the optics). The standard deviation of this reading was 0.67 microns which includes the resolution error of the cameras and the error inherent in the image recognition / position determination routine.

The gap measurement is very sensitive to any contamination on these pins, such as excess grease or condensation onto the cold bar. The software measures the relative x position of the pins by determining the center of gravity of each image. Any droplet of material on any portion of the pin causes an inaccurate reading. The solution so far has to been very aggressive in cleaning the pins after each gap change and vigilantly monitoring the image shown on the screen of the data collection software. This cleaning process takes 5 to 10 minutes after each gap change (with a grease), but this time is not all lost as the system is simultaneously reaching equilibrium.

Parallelism Adjustment

The camera equipment and mechanical systems are described above. The pins are visualized at an angle relative to the turnbuckle height adjustment positions. This angle puts the pins between two pivot points and adjusting the pivot points to obtain parallelism is more difficult. It is less intuitive for the human operator to determine how much each turnbuckle needs to be moved. We have been able to obtain ±5 μm parallelism between the top and bottom meter bars at the beginning of a test. We do see a slight change in parallelism when we lower the hot meter bar during the test to reduce the gap.

CONCLUSIONS

The goal of the ASTM D-5470 test is to measure the thermal impedance of a sample under ideal surface flatness and parallelism conditions to make the test as reproducible as possible by minimizing the interfacial resistance component by measuring temperatures and heat flux carefully. It is well recognized that changing the surface (composition, roughness and flatness) will affect the measured impedance [2,5,15]. There exists some work correlating D5470 test results and actual assembly performance [2], and this is a necessary component for engineers using D5470 results to select materials for a specific design.

The design discussed in this paper successfully increased the precision of impedance measurement by increasing heat flux. We also improved upon the gap and parallelism measurement through use of an optical imaging system. It was found that the optical system requires careful cleaning of the alignment pins to get reproducible gap measurements. Studies have just begun to measure the repeatability and reproducibility of this instrument (multiple tests on the same samples with multiple operators). Future studies will examine the role of meter bar insulation and future improvement in temperature resolution.

REFERENCES

1. Gwin, J. P., M. Saini,, and R. L. Webb. 2002. "Apparatus for Accurate Measurement of Interface Resistance of High Performance Thermal Interface Materials" *Inter Society Conference on Thermal Phenomena*, pp 644–650.
2. Solbrekken, G.L., C-P. Chiu., B. Byers, D. Reichenbacker. 2000. "The Development of a Tool to Predict Package Level Thermal Interface Material Properties", *Inter Society Conference on Thermal Phenomena*, pp 48–54.
3. Kerns, D. 2003. "Improving Accuracy and Flexibility of ASTM D5470 for High Performance Thermal Interface Materials", 19th IEEE SEMI-THERM Symposium Proc, pp 129-133.
4. Kedzierski, M.A., J.L. Worthington III. 1993. "Design and Machining of Copper Specimens with Micro Holes for Accurate Heat Transfer Measurements", *Experimental Heat Transfer*, v6, pp 329–344.
5. Gwinn J.P., R.L. Webb. 2002. "Performance an Testing of Thermal Interface Materials", *Proceedings of THERMES*, pp 201–210
6. "Intel Pentium 4 Processor on a 90 nm Process Datasheet". Available Intel web site, document 30056-002 states that the Prescott processor (1.12 cm^2 die, 9.61 cm^2 integrated heat spreader) uses from 89 to 103 W depending upon the frequency. This calculates to 9.0 to 11 W/cm^2 on the heat spreader surface and calculates to 80 to 92 W/cm^2 on the die surface area.
7. "Standard Test Method for Thermal Transmission Properties of Thin Thermally Conductive Solid Electrical Insulation Materials". *ASTM Test Method D5470-01, Book of Standards Volume 10.02*
8. 300 W steel sheathed Firerod brand cartridge heater, Watlow Electric Manufacturing Company 12001 Lackland Road, St. Louis, Missouri, USA 63146, www.watlow.com
9. Model F25-MB, available from Julabo USA Inc. 754 Roble Road Allentown PA 18109, www.julabo.com.
10. C.Y. Ho, R.W. Powell, E.E. Liley. 1972. "Thermal Conductivity of the Elements", *J. Phys. Chem. Ref. Data, Vol 1, No. 2*, pp 279-421. Copper is listed on page 332.
11. Q912 RTD, available from Logan Enterprises Inc, 8844 US 68 North, PO Box 839, West Liberty OH 43357, www.loganent.com.
12. The DIN 43760 Calibration standard is now maintained as IEC Standard 60751. IEC Central Office 3, rue de Varembé, P.O. Box 131,CH - 1211 GENEVA 20 Switzerland, http://www.iec.ch/index.html. National Instruments incorporates this standard conversion curve into their Measurement and Acquisition software.
13. The meter bars have a lateral surface area of 0.005 m^2 (.0125 m radius and .0635m height). Assuming a natural convection heat transfer coefficient = 10 W/m^2K. For the hot bar the 75°C temperature differential results in 3.5 W, and for the cold meter bar the 30 °C ΔT results in 1.5 W.
14. DVT Corporation, 1855 Satellite Blvd., Suite 100 Duluth, GA 30097-4061 , www.dvtsensors.com
15. Tzeng J. J.-W., T. W. Weber, D. W. Krassowski. 2000. "Technical Review of Thermal Conductivity Measurement Techniques for Thin Thermal Interfaces", 16th IEEE SEMI-THERM Symposium Proc, pp174-181.